Electronic Supplementary Material (ESI) for Journal of Materials Chemistry A.

Fundamental understanding of structure evolution in the synthesis of hard carbon from coal tar pitch for high-performance sodium storage

Lichang Ji [a,d,1], Yun Zhao [a,b,1,*], Lijuan Cao [c], Yong Li [d], Canliang Ma [a], Xingguo Qi [e], Zongping Shao[f,*]

[a] *Institute of Molecular Science, Key Laboratory of Materials for Energy Conversion and Storage of Shanxi Province, Key Laboratory of Chemical Biology and Molecular Engineering of Education Ministry, Shanxi University, Taiyuan 030006, P.R. China*

[b] *Shanxi-Zheda Institute of Advanced Materials and Chemical Engineering, Taiyuan 030006, P.R. China*

[c] *CAS Key Laboratory of Carbon Materials, National Engineering Laboratory for Carbon Fiber Technology, Institute of Coal Chemistry, Chinese Academy of Sciences, Taiyuan, 030001, PR China*

[d] *Research Center for Fine Chemicals Engineering, Shanxi University, Taiyuan 030006, P.R. China*

[e] *Shanxi Huana Carbon Energy Technology Co., Ltd., Taiyuan 030006, P.R. China*

[f] *WA School of Mines: Minerals Energy and Chemical Engineering (WASM-MECE) Curtin University, Perth, WA 6102, Australia*

∗ Corresponding authors.

1 The authors contributed equally to this work.

E-mails: zhaoyun@sxu.edu.cn (Y. Zhao); shaozp@njtech.edu.cn (Z.P. Shao).

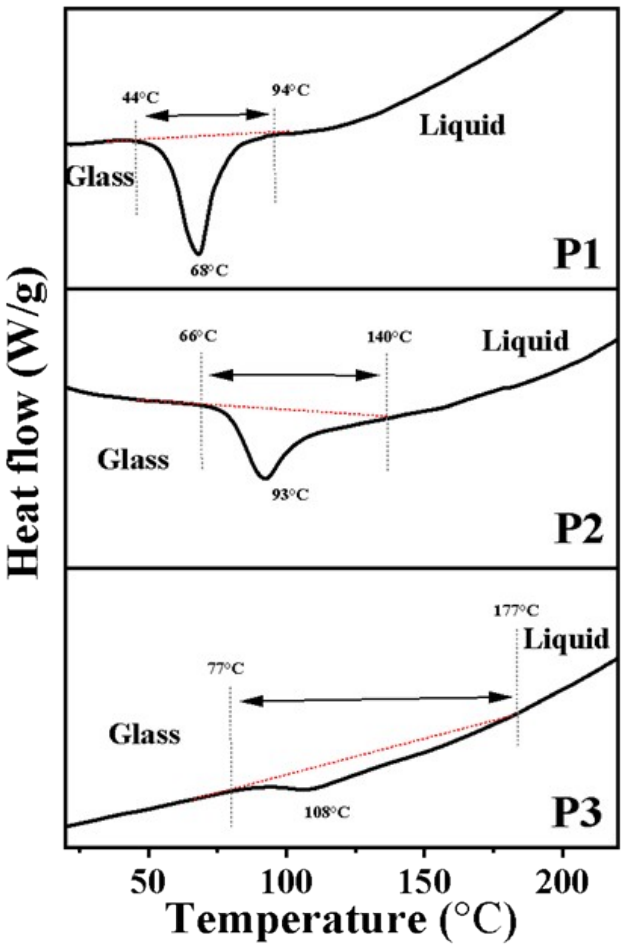

Fig. S1 The DSC curves of P1, P2 and P3.

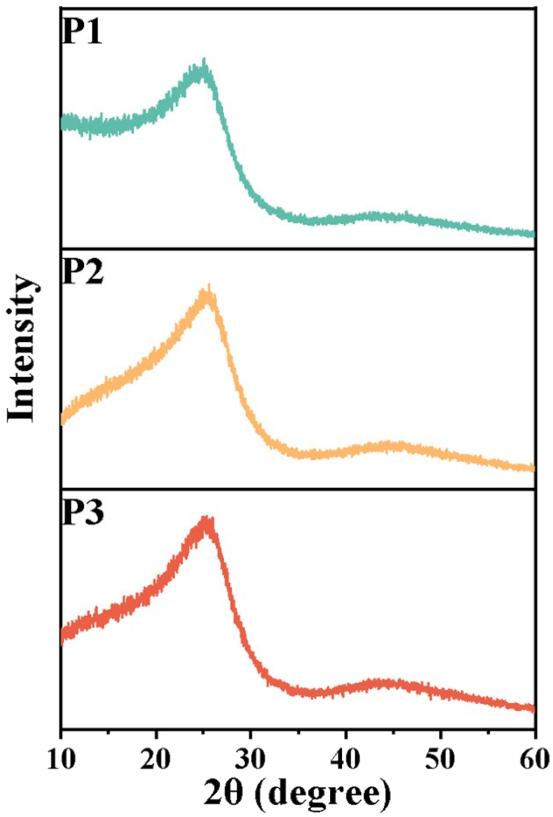

Fig. S2 XRD patterns of CTPs.

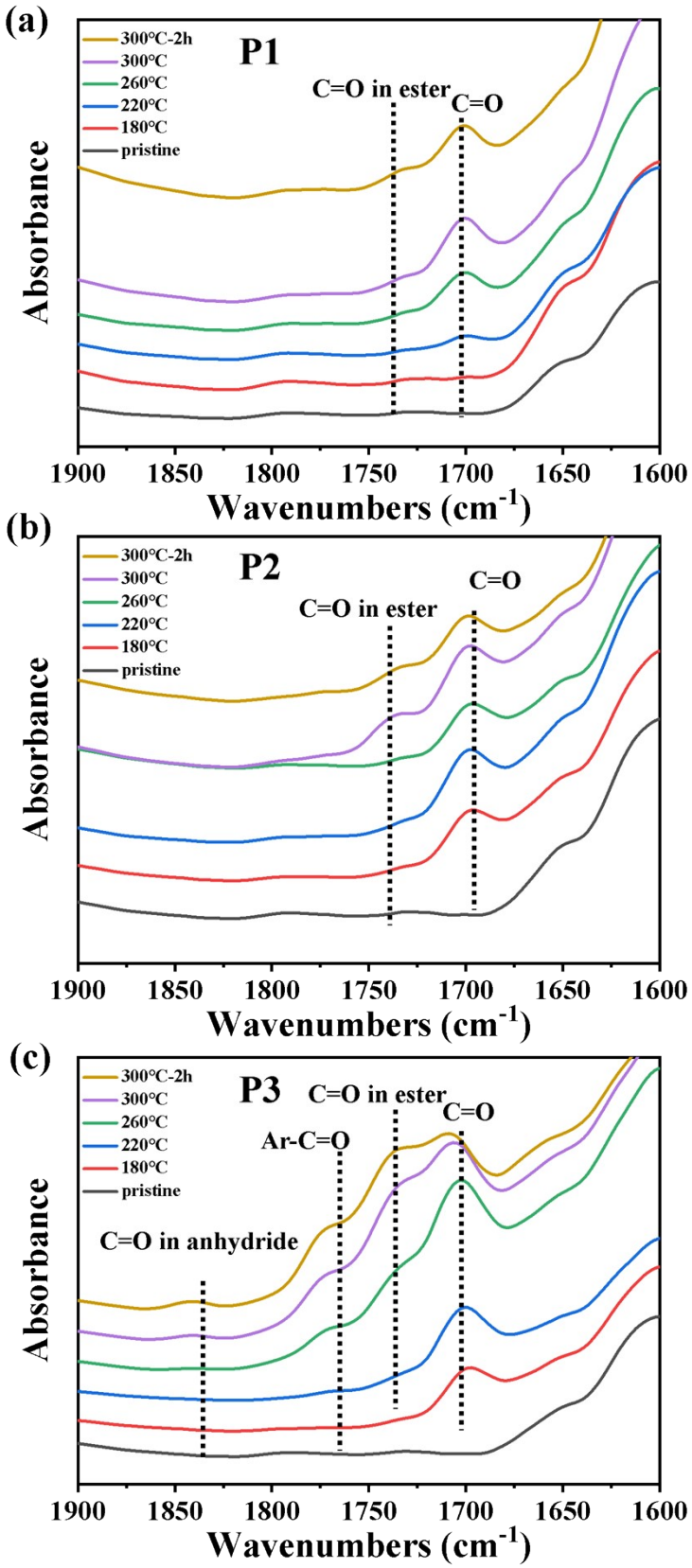

Fig. S3 Ex-situ FTIR spectra of (a) P1 (b) P2 and (c) P3 during the pre-oxidation proccess.

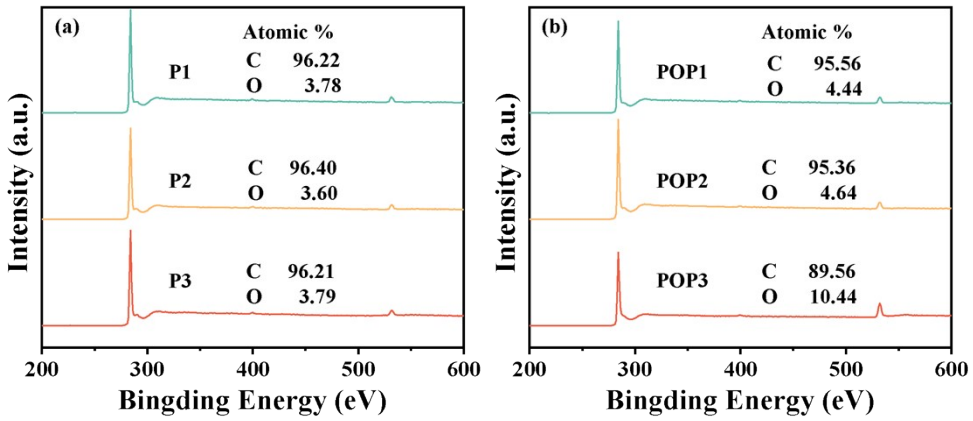

Fig. S4 XPS spectra of (a) pristine CTPs and (b) pre-oxidized CTPs.

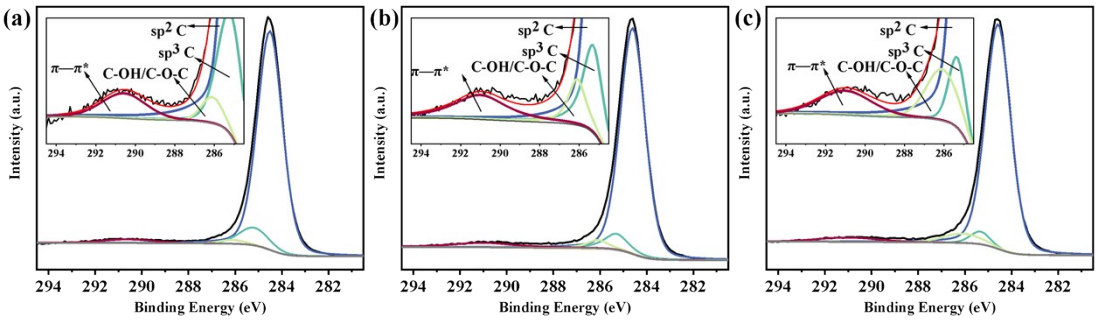

Fig. S5 The fitted XPS C1s profiles of (a) P1, (b) P2, and (c) P3.

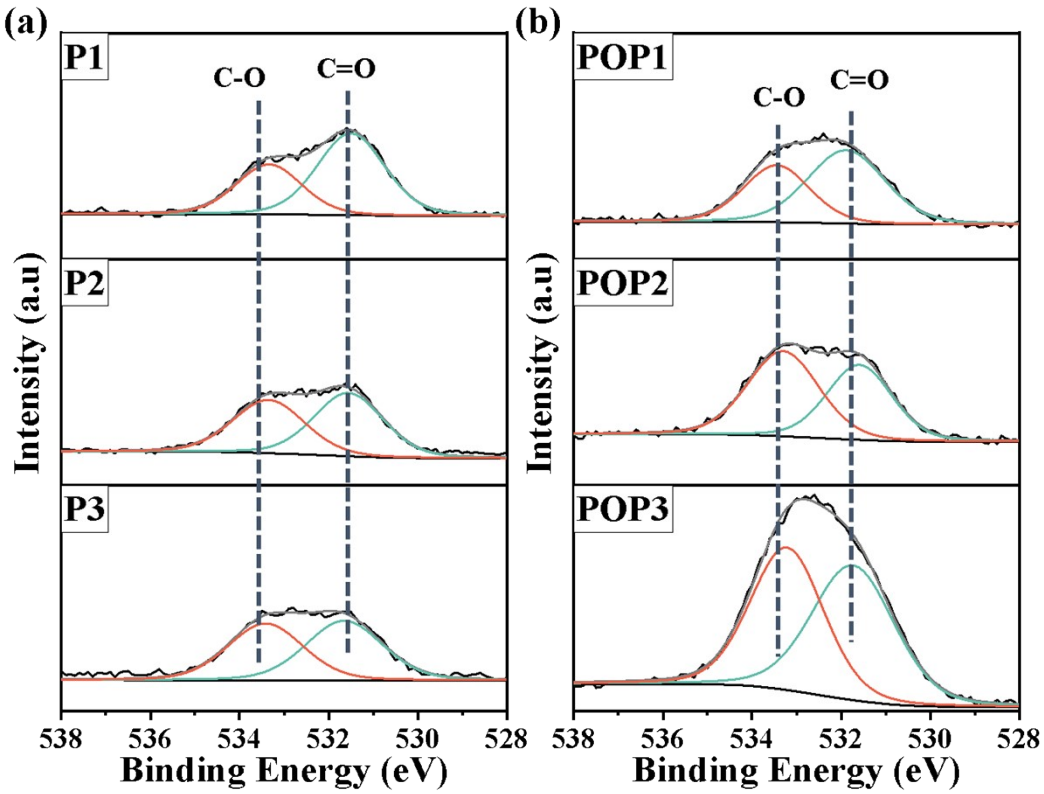

Fig. S6 The fitted XPS O1s profiles of (a) prisine CTPs and (b) pre-oxidized CTPs.

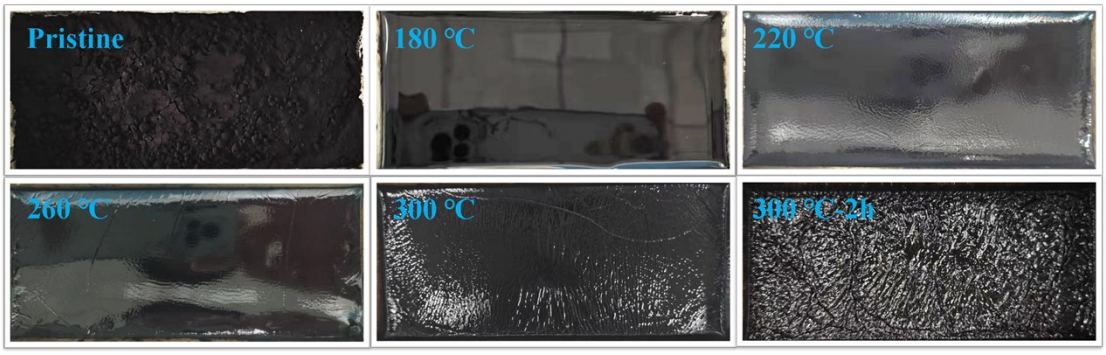

Fig. S7 The ex-situ optical images of P1 at different pre-oxidation stages.

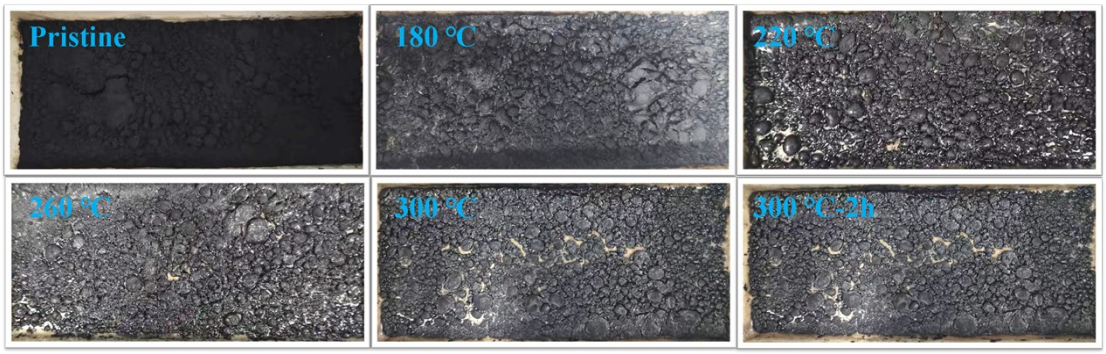

Fig. S8 The ex-situ optical images of P2 at different pre-oxidation stages.

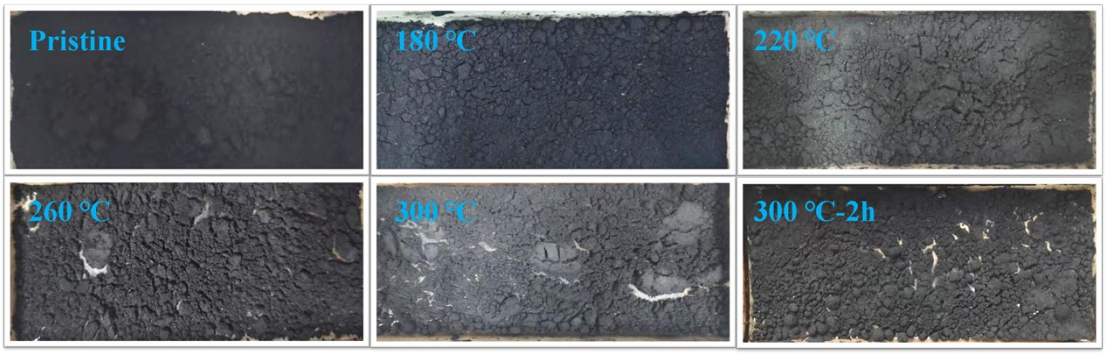

Fig. S9 The ex-situ optical images of P3 at different pre-oxidation stages.

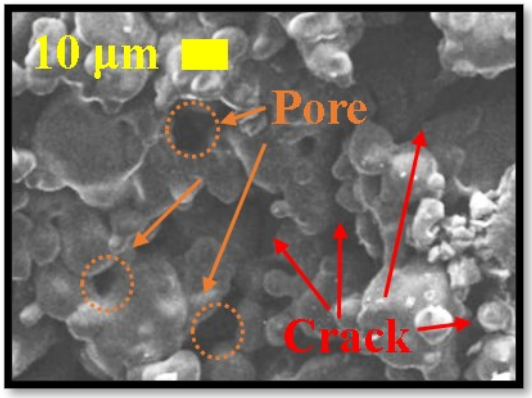

Fig. S10 The magnified SEM image of POP3.

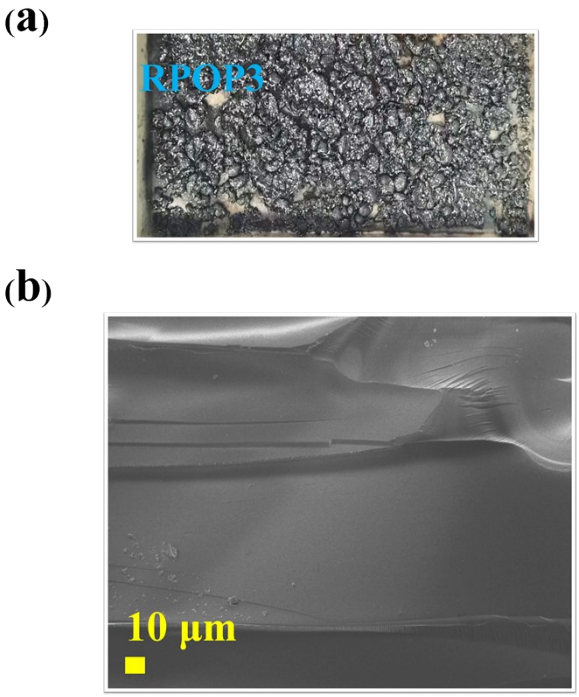

Fig. S11 (a) Optical image and (b) SEM image of RPOP3.

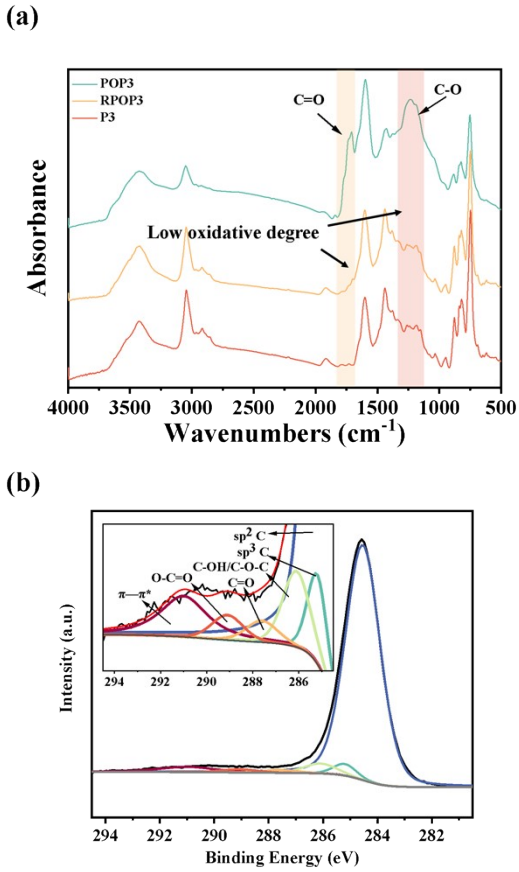

Fig. S12 (a) FTIR spectra of P3, RPOP3 and POP3, (b) The fitted XPS C1s spectrum of RPOP3.

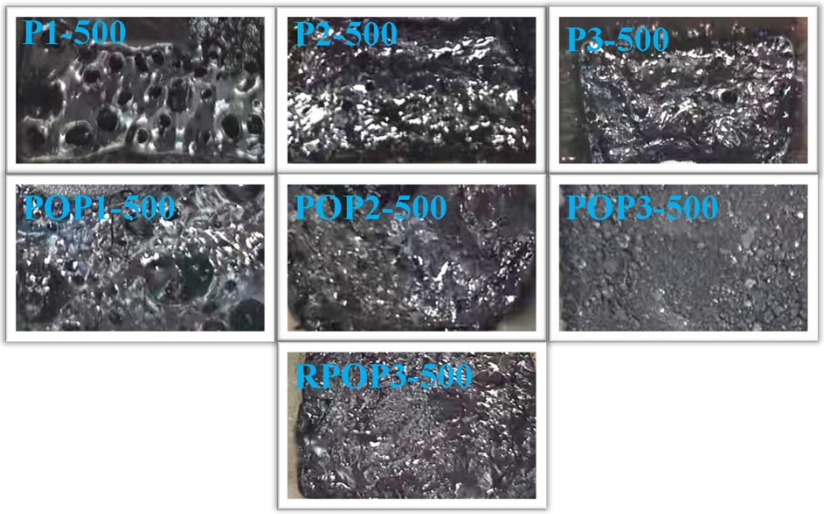

Fig. S13 Optical images of CTPs treated at 500 °C.

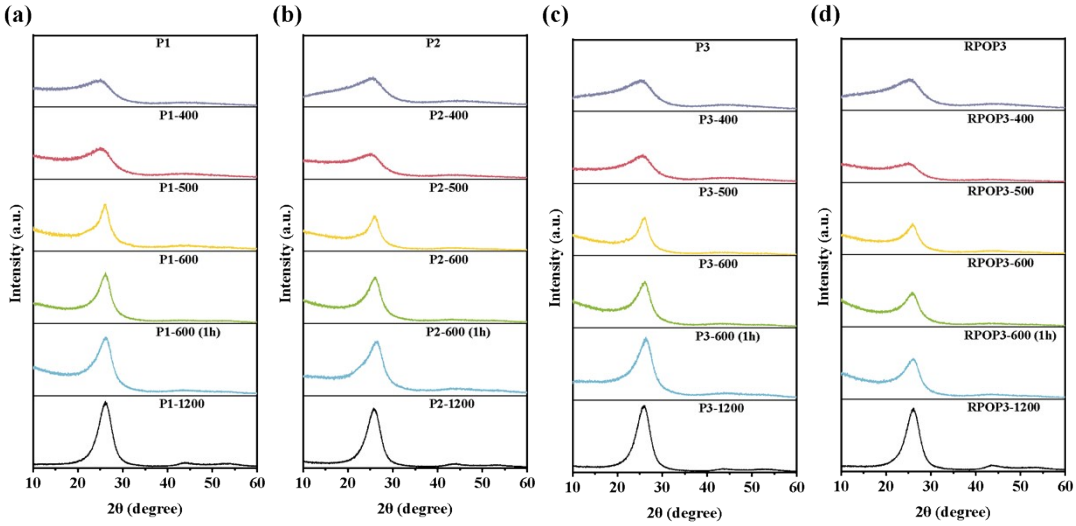

Fig. S14 Ex-situ XRD of (a) P1, (b) P2, (c) P3, and (d) RPOP3 during the carbonization process

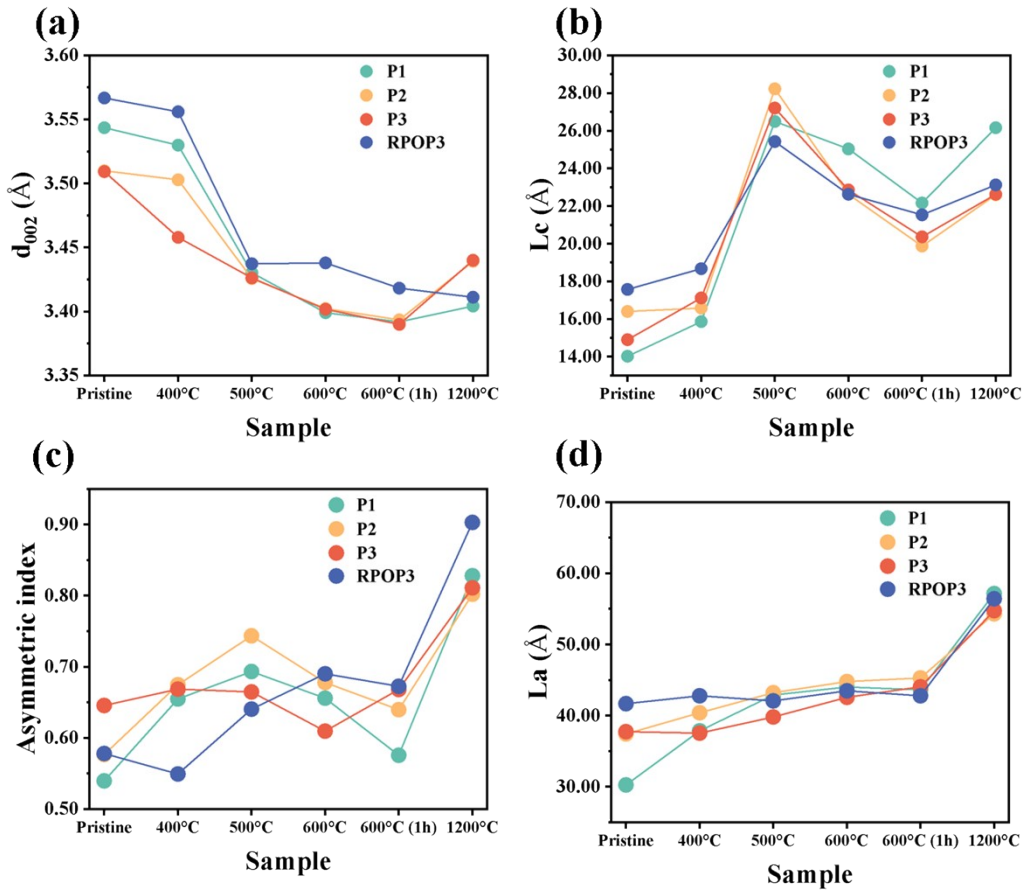

Fig. S15 Variation trends of (a) d_{002} values, (b) Lc values, (c) Asymmetric index, and (d) La values for P1, P2, P3 and RPOP3.

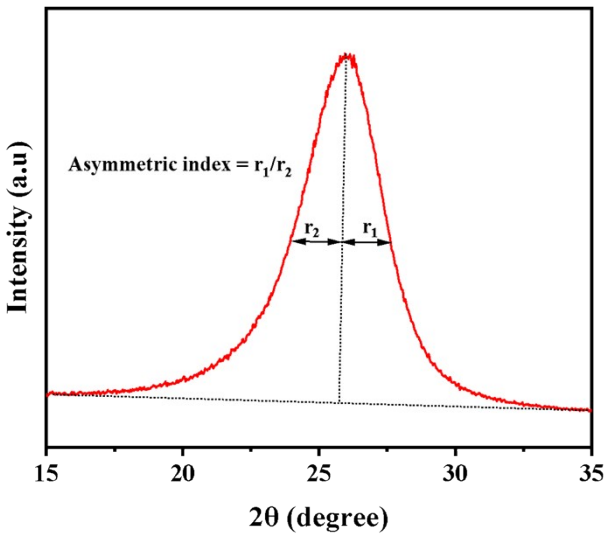

Fig. S16 Illustration of the calculation for asymmetric index (AI).[1]

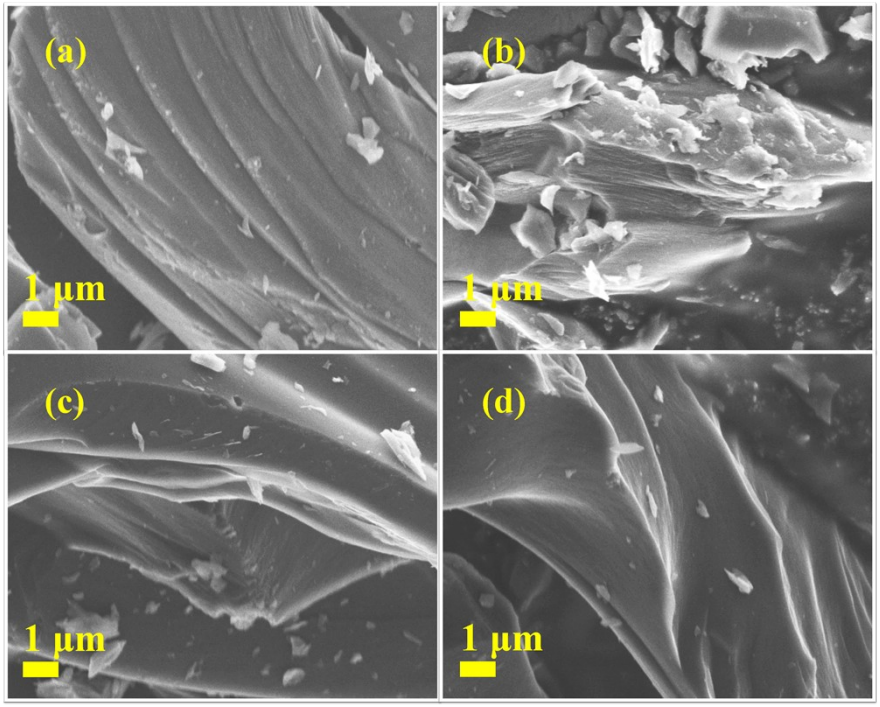

Fig. S17 SEM images of (a) P1-1200, (b) P2-1200, (c)P3-1200 and (d) RPOP3-1200.

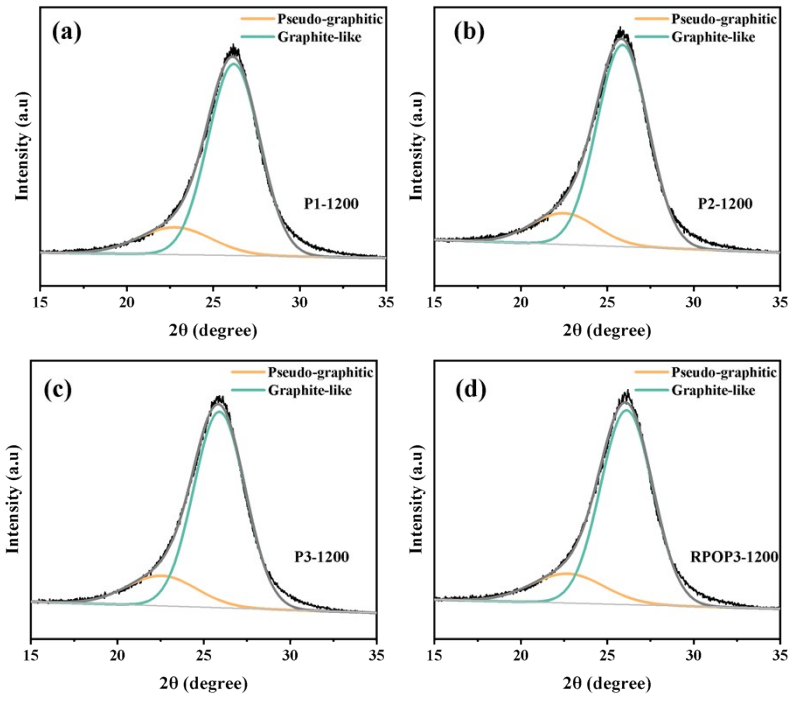

Fig. S18 The fitted XRD results of (a) P1-1200, (b) P2-1200, (c) P3-1200 and (d) RPOP3-1200, respectively.

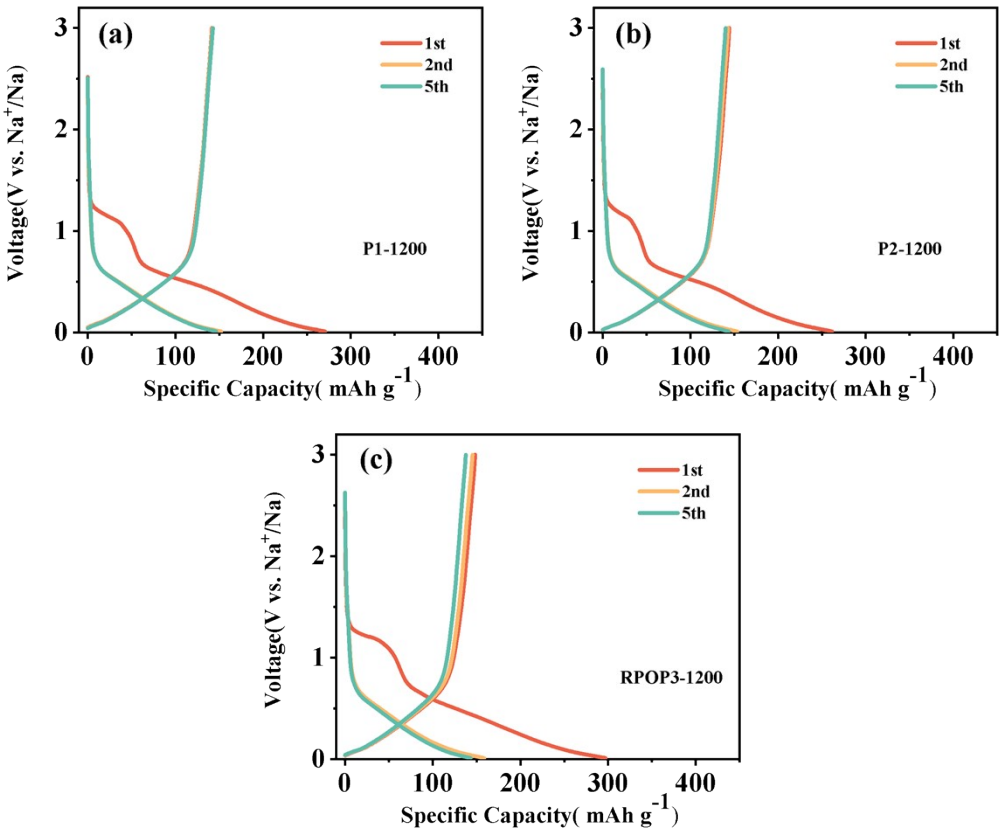

Fig. S19 GCD curves of (a) P1-1200, (b) P2-1200 and (c) RPOP3-1200 at 0.1 C.

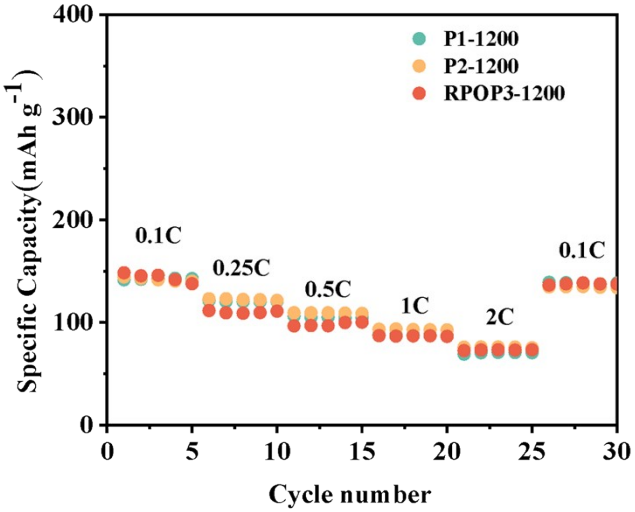

Fig. S20 Rate performance of P1-1200, P2-1200 and RPOP3-1200.

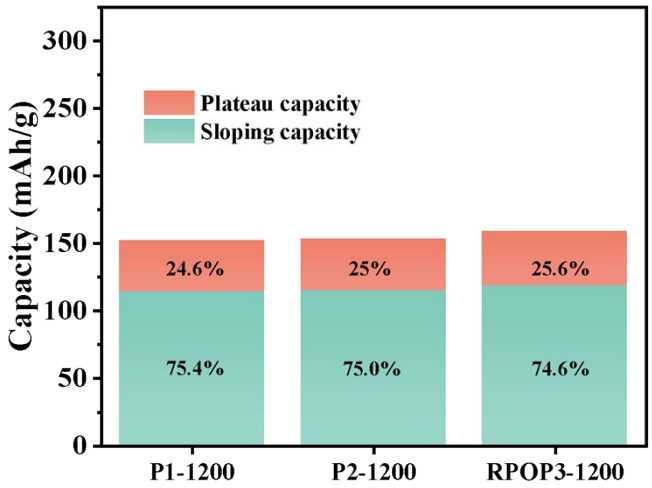

Fig. S21 Slope and plateau contribution from second discharge at 0.1 C of P1-1200, P2-1200 and RPOP3-1200.

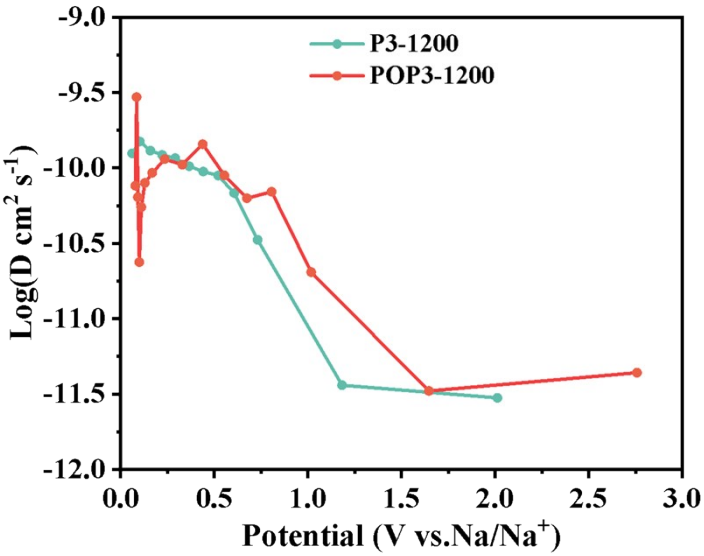

Fig. S22 The Na^+ diffusion coefficients of P3-1200 and POP3-1200 during charge calculated by GITT.

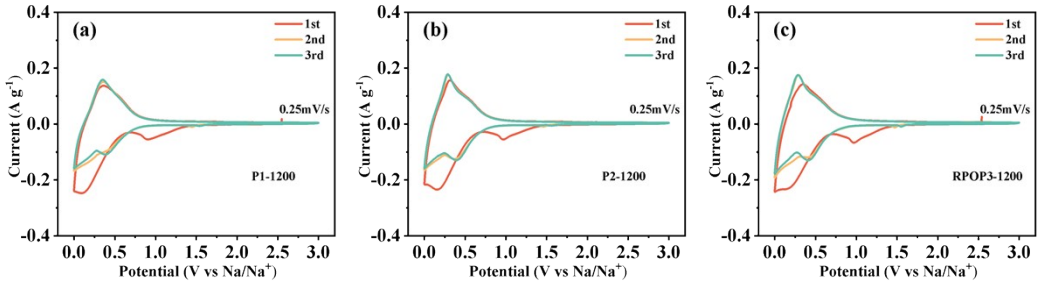

Fig. S23 CV curves of (a) P1-1200, (b) P2-1200 and (c) RPOP3-1200 at 0.25 mv s^{-1}.

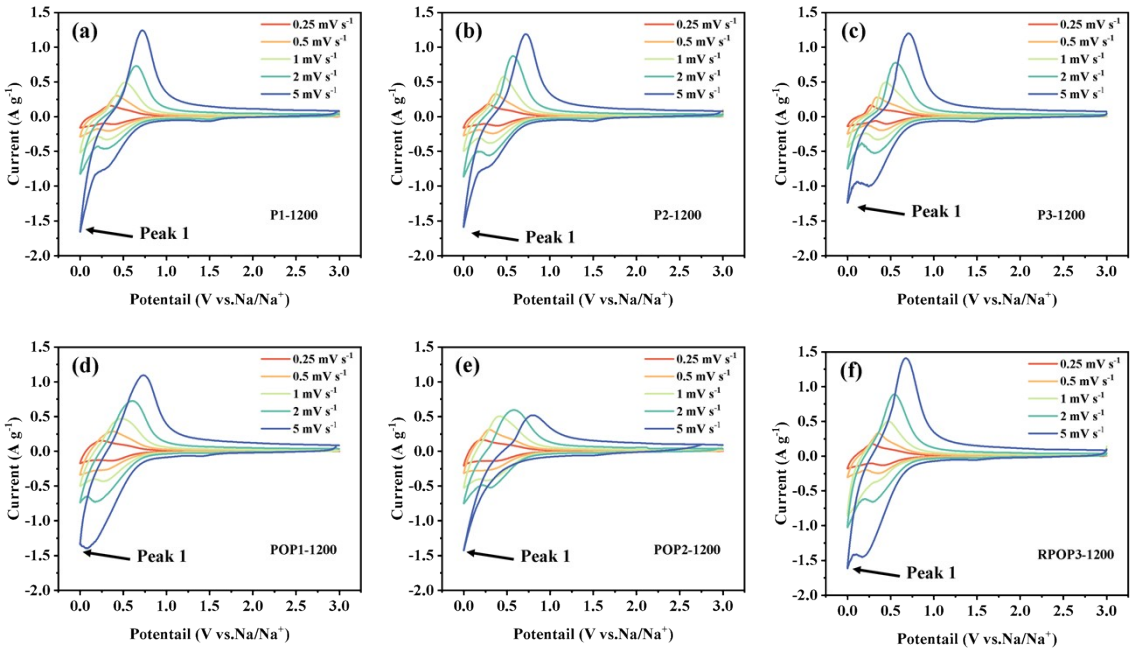

Fig. S24 CV curves of (a) P1-1200, (b) P2-1200, (c) P3-1200, (d) POP1-1200, (e) POP2-1200 and (f) RPOP3-1200 at different scan rate.

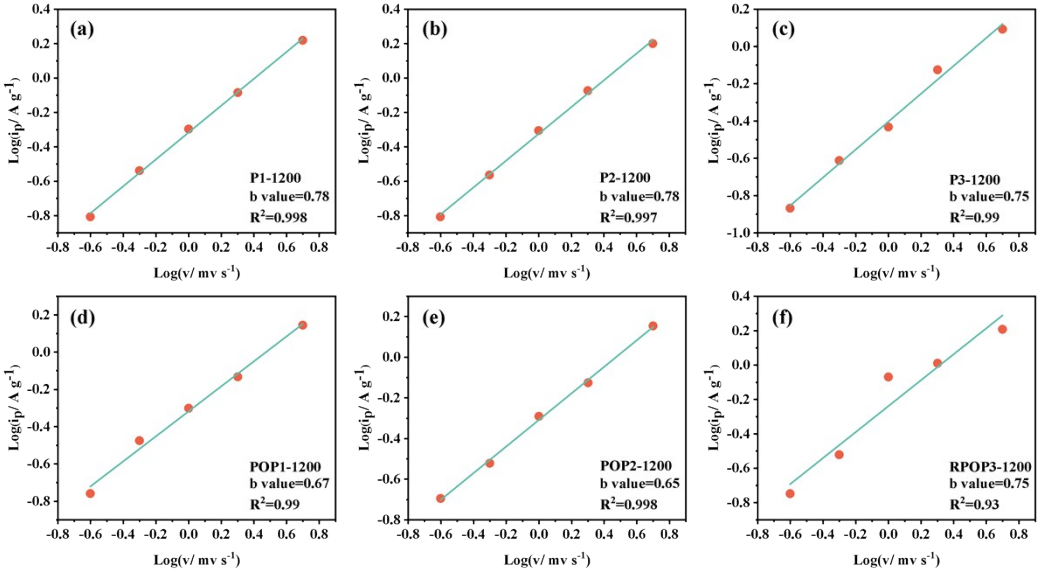

Fig. S25 The correlations of scan rate (v) and peak current (i_p) for (a) P1-1200, (b) P2-1200, (c) P3-1200, (d) POP1-1200, (e) POP2-1200 and (f) RPOP3-1200.

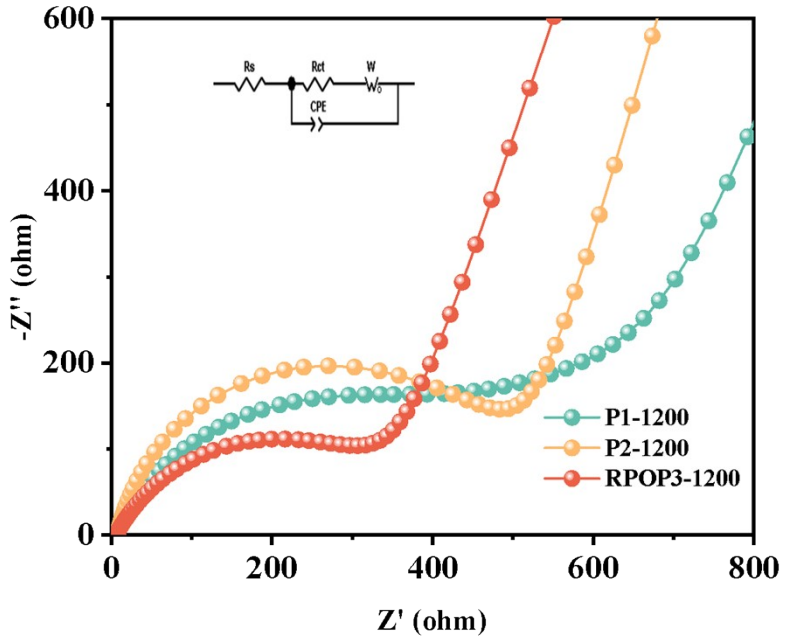

Fig. S26 Nyquist plots of P1-1200, P2-1200 and RPOP3-1200.

Table S1. Assignment details of FTIR spectra.[2]

Group	Position (cm^{-1})	Vibration mode
Aromatic C-H	~3040	Stretching
CH_3	~2953	Asymmetric stretching
CH_2	~2920	Asymmetric stretching
C-H	~2891	Stretching
CH_3	~2870	Symmetric stretching
CH_2	~2850	Symmetric stretching
CH_2 bridging aromatic rings	~2830	Symmetric stretching

Table S2. Structural parameters of pristine CTPs according to XRD.

	γ band/°	π band/°	Aγ	Aπ	far
P1	21.93	25.43	3022.69	3139.92	0.51
P2	20.76	25.65	2497.60	5469.31	0.69
P3	20.52	25.43	1868.12	6100.21	0.77

Table S3. Crystalline parameters of samples according to XRD.

Sample	d002 (Å)	FWHM (002)	Lc (Å)	FWHM (100)	La (Å)
P1	3.5435	5.603	14.02	5.791	30.24
P1-400	3.5289	4.952	15.86	4.615	37.85
P1-500	3.4302	3.04	26.49	4.08	42.89
P1-600	3.399	3.218	25.03	3.966	44.01
P1-600(1h)	3.3919	3.635	22.16	4.007	43.63
P1-1200	3.4012	3.491	23.08	3.066	57.14
P2	3.5099	4.905	16.4	4.673	37.41
P2-400	3.5028	4.848	16.58	4.324	40.4
P2-500	3.4257	2.854	28.22	4.041	43.21
P2-600	3.4023	3.56	22.62	3.902	44.77
P2-600(1h)	3.3934	4.055	19.87	3.867	45.28
P2-1200	3.4391	3.566	22.59	3.224	54.3
P3	3.5092	5.398	14.9	4.626	37.73
P3-400	3.4578	4.699	17.12	4.654	37.53
P3-500	3.4262	2.96	27.2	4.391	39.79
P3-600	3.4017	3.524	22.85	4.101	42.56
P3-600(1h)	3.3899	3.957	20.36	3.968	44.04
P3-1200	3.44	3.56	22.62	3.198	54.75
POP1	3.5567	4.679	17.18	4.022	43.47
POP1-400	3.4526	4.772	16.87	4.138	42.24
POP1-500	3.4113	3.051	26.4	3.803	45.96
POP1-600	3.4094	3.517	22.89	3.861	45.24
POP1-600(1h)	3.3922	3.789	21.21	3.429	50.97
POP1-1200	3.4235	3.425	23.52	2.897	60.42
POP2	3.435	3.656	22.02	4.367	40.01
POP2-400	3.5196	4.911	16.37	4.54	38.5
POP2-500	3.4978	3.93	20.48	4.234	41.25
POP2-600	3.435	3.656	22.02	4.057	43.06
POP2-600(1h)	3.4069	4.325	18.6	4.096	42.72
POP2-1200	3.4264	3.499	23.03	2.855	61.34
POP3	3.6239	4.733	16.97	4.13	42.25

POP3-400	3.5164	4.741	16.95	4.495	38.84
POP3-500	3.554	4.946	16.26	4.118	42.4
POP3-600	3.5868	4.898	16.4	4.06	43.05
POP3-600(1h)	3.6867	4.75	16.92	4.159	42.03
POP3-1200	3.7718	4.846	16.91	3.836	45.69
RPOP3	3.5667	4.578	17.57	4.202	41.67
RPOP3-400	3.5559	4.306	18.67	4.084	42.78
RPOP3-500	3.4372	3.167	25.42	4.156	42.06
RPOP3-600	3.4379	3.56	22.62	4.015	43.47
RPOP3-600(1h)	3.4182	3.74	21.53	4.088	42.77
RPOP3-1200	3.4111	3.485	23.12	3.105	56.41

Table S4. Physical parameters of CTP-derived carbons according to XRD.

sample	Disordered			Pseudo-graphitic			Graphite-like		
	2θ/°	d002/Å	Area/%	2θ/°	d002/Å	Area/%	2θ/°	d002/Å	Area/%
P1-1200	-	-	-	22.78	3.90	16.65	26.18	3.40	83.35
P2-1200	-	-	-	22.49	3.95	16.37	25.88	3.44	83.63
P3-1200	-	-	-	22.57	3.94	17.15	25.91	3.44	82.85
POP1-1200	-	-	-	22.68	3.92	14.21	25.98	3.43	85.79
POP2-1200	-	-	-	22.66	3.92	13.15	25.96	3.43	86.85
POP3-1200	19.17	4.63	6.48	23.19	3.83	70.22	26.24	3.39	23.30
RPOP3-1200	-	-	-	22.70	3.91	17.35	26.12	3.41	82.65

Table S5. Assignments of Raman spectra.[3]

Band	Raman shift（cm^{-1}）	Vibration mode	Structure	Line shape
G	~1590	E2g symmetry	Ideal graphitic lattice	Lorentzian
D (D1)	~1350	A1g symmetry	Graphene layer edges	Lorentzian
D2	~1620	E2g symmetry	Surface graphene layers	Lorentzian
D3	~1500		Amorphous carbon	Gaussian
D4	~1200	A1g symmetry	sp2-sp3 bonds or C–C and C=C stretching vibrations	Lorentzian

Table S6. Electrochemical performance comparison between POP3-1200 and other pitch-derived carbons

Materials	Capacity	rate capacity	Cyclability	Electrolyte	ICE

	(mAh g^{-1}/mA g^{-1})	(mAh g^{-1}/mA g^{-1})			(%)
This work	276.8/30	87 / 2C	91.2% after 500 cycles	1 M $NaClO_4$ in DMC/ EC/EMC with 2% FEC	67.50
Pre-oxidized pitch derived carbon[4]	300.83/20	~60 / 500	~73% after 100 cycles	1M $NAClO_4$ in EC/DEC	82.82
Pre-oxidized pitch derived carbon[5]	300.6/30	~77 / 2C	93.1% after 200 cycles	1M $NaPF_6$ in EC/DMC	88.60
Pitch derived 3D porous carbon[6]	215/50	97 / 5000	93% after 120 cycles	1M $NAClO_4$ in EC/DMC	60
Pitch derived carbon solidified by $Mg(NO_3)_2$▪$6H_2O$[7]	278/30	74/ 2C	98% after 300 cycles	1M $NaPF_6$ in EC/DMC	/
Pitch derived carbon via nanocasting[8]	130/0.2C	~120/2C	/	1M $NaPF_6$ in EC/DMC	/
N,P-doped pitch derived carbon[9]	285/100	140/5000	82% after 100 cycles	1MNAClO_4 in EC/DMC	42.1
Pitch derived Hard–Soft Carbon Composite[10]	282/30	~80/1200	85% after 100 cycles	1M $NaClO_4$ in EC/DMC	80
Pitch derived soft carbon[11]	263/0.15C	124 /3600	70% after 500 cycles	1MNaPF_6 in EC/DMC	80

Table S7. Fitting results of Nyquist plots.

Sample	R_s(Ω)	R_{ct}(Ω)
P1-1200	5.044	405.9
P2-1200	7.484	434.4
P3-1200	6.866	246.1
POP1-1200	7.897	299.8
POP2-1200	6.696	494.3
POP3-1200	7.575	494.7
RPOP3-1200	5.359	377.9

References

1 S. Zhang, Q. Liu, H. Zhang, R. Ma, K. Li, Y. Wu and B. J. Teppen, *Carbon*, 2020, **157**, 714–723.

2 C. Russo, F. Stanzione, A. Tregrossi and A. Ciajolo, *Carbon*, 2014, **74**, 127–138.

3 A. Sadezky, H. Muckenhuber, H. Grothe, R. Niessner and U. Pöschl, *Carbon*, 2005, **43**, 1731–1742.

4 R. Xu, Z. Yi, M. Song, J. Chen, X. Wei, F. Su, L. Dai, G. Sun, F. Yang, L. Xie and C.-M. Chen, *Carbon*, 2023, **206**, 94–104.

5 Y. Lu, C. Zhao, X. Qi, Y. Qi, H. Li, X. Huang, L. Chen and Y.-S. Hu, *Adv. Energy Mater.*, 2018, **8**, 1800108.

6 D. Qiu, T. Cao, J. Zhang, S.-W. Zhang, D. Zheng, H. Wu, W. Lv, F. Kang and Q.-H. Yang, *Journal of Energy Chemistry*, 2019, **31**, 101–106.

7 Y. Qi, Y. Lu, L. Liu, X. Qi, F. Ding, H. Li, X. Huang, L. Chen and Y.-S. Hu, *Energy Storage Materials*, 2020, **26**, 577–584.

8 S. Wenzel, T. Hara, J. Janek and P. Adelhelm, *Energy Environ. Sci.*, 2011, **4**, 3342.

9 C. Gao, J. Feng, J. Dai, Y. Pan, Y. Zhu, W. Wang, Y. Dong, L. Cao, L. Guan, L. Pan, H. Hu and M. Wu, *Carbon*, 2019, **153**, 372–380.

10 F. Xie, Z. Xu, A. C. S. Jensen, H. Au, Y. Lu, V. Araullo-Peters, A. J. Drew, Y. Hu and M. Titirici, *Adv. Funct. Mater.*, 2019, **29**, 1901072.

11 Y. Qi, Y. Lu, F. Ding, Q. Zhang, H. Li, X. Huang, L. Chen and Y. Hu, *Angew. Chem.*, 2019, **131**, 4405–4409.